Cancer Management and Research

Dovepress
open access to scientific and medical research

Open Access Full Text Article

ORIGINAL RESEARCH

Differential diagnostic value of ^{18}F-FDG PET/CT for benign and malignant vertebral compression fractures: comparison with magnetic resonance imaging

This article was published in the following Dove Press journal:
Cancer Management and Research

Xiaojiang He[1,*]
Long Zhao[1,*]
Xiuyu Guo[1]
Liang Zhao[2]
Jing Wu[1]
Jingxiong Huang[1]
Long Sun[1]
Chengrong Xie[3]
Haojun Chen[1]

[1]Department of Nuclear Medicine and Minnan PET Center, Xiamen Cancer Hospital of the First Affiliated Hospital of Xiamen University, Xiamen 361003, China; [2]Department of Radiation Oncology, Xiamen Cancer Hospital of the First Affiliated Hospital of Xiamen University, Xiamen 361003, China; [3]Department of Hepatobiliary Surgery, Fujian Provincial Key Laboratory of Chronic Liver Disease and Hepatocellular Carcinoma, Xiamen 361004, China

*These authors contributed equally to this work

Purpose: The purpose of this study was to evaluate the differential diagnostic value of 2-[fluorine-18]-fluoro-2-deoxy-D-glucose (^{18}F-FDG) positron emission tomography (PET)/computed tomography (CT) for benign and malignant vertebral compression fractures (VCFs), where the diagnostic accuracy of ^{18}F-FDG PET/CT was compared with magnetic resonance imaging (MRI).

Patients and methods: Between 2015 and 2017, we retrospectively evaluated 87 patients with 116 VCFs. MRI was performed in all the 87 patients, whereas ^{18}F-FDG PET/CT was executed in 51 patients. Three malignant features (convex posterior cortex, epidural mass formation, and pedicle enhancement) from MRI and the maximum standardized uptake value (SUV_{max}) from ^{18}F-FDG PET/CT were evaluated in benign and malignant VCFs, respectively. Sensitivity, specificity, positive predictive value, and negative predictive value of MRI and ^{18}F-FDG PET/CT were compared in the differentiation of malignant from benign VCFs.

Results: The results of our investigation showed that the sensitivity and specificity for predicting malignant VCFs were 75.6% and 77.3% for convex posterior cortex, 82.9% and 813% for epidural mass formation, and 85.7% and 70.8% for pedicle enhancement. ^{18}F-FDG PET/CT demonstrated higher sensitivity (100%) but lower specificity (38.9%) as compared to MRI with regard to differentiation between benign and malignant VCFs. A significant difference in the SUV_{max} values was observed between the benign and malignant fractures (2.9 ± 1.0 vs 5.0 ± 1.8, $P < 0.01$). Besides the value of SUV_{max}, it has been noticed that the FDG uptake pattern differed in malignant and benign fractures.

Conclusion: Significant MRI findings such as convex posterior cortex, epidural mass formation, and pedicle enhancement are highly suggestive of malignancy. ^{18}F-FDG PET/CT reliably differentiated the fractures of malignant from benign based on both SUV_{max} and ^{18}F-FDG uptake pattern. In a situation where MRI findings are not diagnostic, ^{18}F-FDG PET/CT provides additional information as it has high sensitivity and is semiquantitative.

Keywords: vertebral compression fractures, MRI, ^{18}F-FDG PET/CT, maximum standardized uptake value

Introduction

Vertebral compression fractures (VCFs) are common in the elderly, particularly in those who are osteoporotic.[1] Such fractures include benign and pathological; the former is usually due to osteoporosis, while the latter is mainly due to vertebral metastasis or myeloma. The vertebral column is a region of the skeleton most frequently affected by metastatic diseases in cancer patients. Signs of neurologic dysfunction may be

Correspondence: Haojun Chen
Department of Nuclear Medicine and Minnan PET Center, Xiamen Cancer Hospital of the First Affiliated Hospital of Xiamen University, 55 Zhenhai Road, Xiamen, Fujian 361003, China
Tel/fax +86 592 213 7077
Email leochen0821@foxmail.com

submit your manuscript | www.dovepress.com
Dovepress
http://dx.doi.org/10.2147/CMAR.S168374

nonspecific with both types of fracture, and back pain may be the only complaint. Therefore, it is very important to differentiate benign VCFs from malignant fractures, particularly in elderly patients who have a history of malignancy.[2]

Traditional imaging modalities such as radiography and computed tomography (CT) play a very important role in the diagnosis and differentiation of conditions involving bones fractures.[3] However, such imaging modalities may not always be possible to differentiate the fractures of malignant from benign.[4] Bone scintigraphy has been widely used in the screening of skeletal metastasis, but a bone scan remains positive for many years after bone fracture, where distinguishing the nature of bone fracture may be challenging.[5] Recently, magnetic resonance imaging (MRI) has been used for evaluating the bones fractures. On both T1- and T2-weighted images, normal bone marrow has a characteristic signal intensity that can often be distinguished from the intensity of a pathological process.[6] In addition, the morphological features of collapsed vertebrae may be used as reliable MRI criteria for the differentiation between benign and malignant fractures. Three typical radiological features of MRI indicating the malignant fractures are pedicle involvement, convex posterior cortex, and paraspinal or epidural mass formation.[7] Although sensitivity, specificity, and diagnostic accuracy have been reported for each feature, the pathognomonic MRI finding for malignant VCFs remained unclear. Recently, diffusion-weighted magnetic resonance imaging (DWI or DW-MRI) has been reported to be useful for probing the structure of biological tissues at a microscopic level and can be used in the differentiation between benign and malignant VCFs.[8] However, some overlap between the ranges in the values of the apparent diffusion coefficient (ADC) for benign and malignant lesions was observed, which poses some limitations for such differentiation in some of the cases.[9,10]

Positron emission tomography (PET) employing a glucose analogue tracer, 2-[fluorine-18]-fluoro-2-deoxy-D-glucose (^{18}F- FDG), has been widely used to diagnose and grade malignant disease.[11] PET/computed tomography (PET/CT), as an integrated system combining PET and CT in the same session, has been proven to be a useful tool for improving the diagnostic performance of neoplasms.[12] Although the spatial and temporal resolution of PET may not be as impressive as other imaging modalities, its sensitivity is exquisite.[13] In terms of the VCFs, an increased FDG uptake can always be observed in the malignant fractures but not in the fractures caused by osteoporosis. Another advantage of PET for identifying malignancy is the relatively easy process of quantitative analysis. The most common PET parameter for quantifying the tracer uptake is the maximum standardized uptake value (SUV_{max}), which is the ratio of the concentration of image-derived radioactivity to the concentration of the injected radioactivity in the whole body. However, there is no generalized consensus on the cutoff value of SUV_{max} for differentiating malignancy from benignity with ^{18}F-FDG PET/CT. So far in the literature, very few comparative studies between MRI and ^{18}F-FDG PET/CT were reported regarding the differential diagnostic value for benign and malignant VCFs.

On this context, the aim of this investigation was to evaluate the differential diagnostic value of ^{18}F-FDG PET/CT for benign and malignant VCFs, and the diagnostic efficacy of ^{18}F-FDG PET/CT was compared with that of MRI. Also, the best SUV_{max} cutoff value from ^{18}F-FDG PET/CT that can reliably differentiate malignant VCFs from benignity was determined. Overall, through this investigation, a reliable diagnostic algorithm in VCF patients with suspected malignancy has been proposed.

Patients and methods

Patients

Between 2015 and 2017, we retrospectively evaluated the hospital charts and diagnostic studies of patients with VCFs imaged with MRI. Subjects were excluded from this study if they had history of simple traumas. The final study group consisted of 87 patients: 55 males and 32 females (mean age: 68 years; age range: 60−79 years), with a total of 116 compressed vertebral bodies. Forty-two cases did not have any primary malignancy, whereas 45 cases had histories of malignant tumors (these patients were considered as cancer patients). The primary sites of these malignancies were esophageal cancer (n = 2), stomach cancer (n = 3), hepatic cancer (n = 3), colon cancer (n = 5), breast cancer (n = 12), and lung cancer (n = 20). ^{18}F-FDG PET/CT scans were carried out in 51 patients, including 45 cancer patients. Regarding the other six patients with no history of malignant tumors, ^{18}F-FDG PET/CT was performed as MRI findings were not diagnostic and the VCFs lesions were observed at multiple levels.

PET/CT-guided percutaneous vertebral biopsy was performed in 28 patients, and the final diagnosis was based on the results of histopathological examination. Regarding the other 59 patients who did not receive vertebral biopsy, the final diagnosis was made primarily by means of follow-up radiological examinations in combination with clinical history. A minimum follow-up time of 24 months was required

in patients with negative follow-up radiological examinations. When the appearance of follow-up radiological studies did not improve or significantly change in a patient without a clinical history of malignancy, the fracture was considered to be caused by a benign trauma, where osteoporosis was considered to be the most likely cause of the fracture. On the other hand, a diagnosis of traumatic fracture was made when there was a history of trauma and improvement in the follow-up studies. When a patient (especially those with a known primary malignancy) showed progressive deterioration of vertebral fractures or involvement of other vertebrae during the follow-up radiological examinations, the fracture was considered to be malignant compression fracture. Finally, all the patients were divided into two groups based on the final diagnosis: benign and malignant fracture groups. This study protocol was discussed and agreed by the Medical Ethics Committee of the Xiamen Cancer Hospital of the First Affiliated Hospital of Xiamen University and all the patients were informed and provided with a written consent.

PET/CT and MRI acquisition protocol

All the patients were required to fast for at least 6 h before performing the examination. Serum glucose levels of all the patients were below 150 mg/dL. The dose of intravenously injected ^{18}F-FDG was calculated according to the patient's weight (3.7 MBq [0.1 mCi]/kg]). Data were acquired with a PET/CT system (Discovery ST; GE Medical Systems, Waukesha, WI, USA) after 1 h of injection. The parameters for the acquisition were as follows. CT scanning (140 kV, 120 mA, a tube rotation time of 0.5 s, a pitch of 6, and a section thickness of 3.75 mm) was at first performed from the base of skull to the upper thigh. A PET scan was performed immediately after CT acquisition, where the acquisition was in 3-D mode. The time of acquisition was 3 min per position. All the obtained data were transferred to the Xeleris workstation; data were reconstructed using the ordered subset expectation maximization algorithm, using CT data for attenuation correction, and the reconstructed images were then co-registered and displayed.

MR imaging was performed with a 3.0-T superconducting MRI system (Magnetom Verio Tim; Siemens Healthcare, Erlangen, Germany). Sagittal and axial, relatively 0.6 cm thick, T1-weighted images were obtained with a spin-echo technique (repetition time [ms]/echo time [ms] = 250/2.48). Sagittal, relatively 0.6 cm thick, T2-weighted (6000/96) images were also obtained routinely. Additional pulse sequences and imaging planes with varying section thicknesses were obtained in certain cases.

PET/CT and MR imaging analysis

Fused PET/CT images, including coronal, sagittal, and transaxial reformations, were viewed on the Xeleris workstation. Two experienced nuclear medicine physicians, who were blinded to the clinical history and or pathological results of the patients, performed a consensus review. Region of interests were drawn on transaxial images around the involved vertebra, which were confirmed on sagittal images for the purpose of semiquantitative analysis. The SUV_{max} values were automatically calculated, which were used to quantify the uptake of FDG in the corresponding vertebra.

Diagnostic standard with ^{18}F-FDG PET/CT: a semiqualitative assessment was made with the specific aim of establishing whether the lesion was benign or malignant. ^{18}F-FDG uptake in the lesion was compared with that in the liver, and those lesions with uptake greater than that in the liver were regarded as malignancy. Besides the metabolic information, the paravertebral soft tissue mass and spinal accessory involvement observed from additional CT imaging are also indicative of malignant compression fractures.

The MR studies were reviewed independently by two experienced radiologists without the knowledge of clinical history or pathological results. Reliable MRI criteria for identifying the malignant or benign VCFs was based on the changes in the signal intensity as well as the morphological features of the compressed vertebrae.[7] It has been reported that all the malignant lesions appeared as low-intensity areas on T1-weighted images, and 50% of the non-neoplastic lesions (including osteoporotic fractures) also appeared in this way. As such, the signal intensity may be of little use in distinguishing malignant lesions from non-neoplastic ones and therefore not discussed in this study. Three typical radiological features of MRI indicating the malignant compression fractures are: 1) convex posterior cortex on sagittal view, 2) epidural or paraspinal mass formation on axial view, and 3) pedicle enhancement on axial view (after Gd-DTPA injection).

In this study, three malignant findings on MRI were evaluated in all the patients, and SUV_{max} and FDG uptake pattern were evaluated in patients who underwent PET/CT scans. The prevalence of each malignant finding was compared between the benign and malignant groups. The sensitivity, specificity, positive predictive value (PPV) and negative predictive value (NPV) of each malignant finding were calculated and compared to evaluate the diagnostic efficacy. In cases where all the three malignant features were observed, the diagnostic efficacy of this finding was also evaluated. On the other hand, the relationship between SUV_{max} and malignancy was

evaluated to determine the cutoff value of SUV_{max} which can most reliably differentiate malignant VCFs from benignity.

Statistical analysis

Statistical analysis was performed with SPSS software 13.0 (SPSS, Inc.). Differences between the paired parameters were tested by Wilcoxon signed-rank or *t*-test. The sensitivity, specificity, PPV, and NPV of MRI and PET findings were calculated and compared. A receiver operating characteristic curve (ROC curve) analysis was performed to identify the optimal cutoff value of PET parameter (SUV_{max}) for the differentiation between benignity and malignancy. Statistical analysis was performed by using an unpaired *t*-test, and *P*-values less than 0.05 were considered statistically significant. All statistical tests were two-sided, and *P*-values of less than 0.05 were considered statistically significant.

Results

Characteristics of patients and outcomes

In this investigation, a total of 87 patients were considered and the characteristics of patients are shown in Table 1. Fifty-seven patients had single vertebral involvement, and the remainder had multiple vertebrae involvement. In total, 116 vertebrae among 87 cases were investigated, and the lesion sites involved thoracic vertebrae (n = 64) and lumbar vertebrae (n = 52). The involved vertebral body levels ranged from T6 to L5. More specifically, the thoracic vertebrae were T6 (n = 3), T7 (n = 9), T8 (n = 12), T9 (n = 12), T10 (n = 3), T11 (n = 10), and T12 (n = 15), while the lumbar vertebrae were L1 (n = 13), L2 (n = 12), L3 (n = 5), L4 (n = 7), and L5 (n =15). The final diagnosis involved 41 malignant compression fractures (in 37 patients) and 75 benign compression fractures (in 50 patients). Thirty-seven patients in the malignant fracture group included 34 cancer patients and 3 non-cancer patients (patients with plasma cell myeloma), while the other 50 patients in the benign fracture group consisted of 11 cancer patients and 39 non-cancer patients. Regarding the shape of VCFs, the number of wedge-shaped, flat-shaped, and concave-shaped VCFs were 18, 34, and 23 in the benign fracture group, whereas 9, 18, and 14 in the malignant fracture group, respectively. There is no statistical difference regarding the vertebral shape between the benign and malignant VCFs ($P > 0.05$).

Table 1 Patient characteristics

Characteristics	Number of cases (%)
Age (years)	
Mean	68
Range	60–79
Sex (patients)	
Male	55 (63.2)
Female	32 (36.8)
Lesion sites (lesions)	
Thoracic vertebrae	64 (55.2)
T6	3
T7	9
T8	12
T9	12
T10	3
T11	10
T12	15
Lumbar vertebrae	52 (44.8)
L1	13
L2	12
L3	5
L4	7
L5	15
Final diagnosis (lesions)	
Osteoporosis (50 patients)	75 (64.6)
Vertebral metastasis (34 patients)	38 (32.8)
Plasma cell myeloma (3 patients)	3 (2.6)
Vertebra involvement (patients)	
Single	57 (65.5)
Multiple	30 (34.5)
History of malignancy (patients)	
Without malignancy	42 (48.3)
History of malignant tumor	45 (51.7)
Lung cancer	20
Breast cancer	12
Colon cancer	5
Hepatic cancer	3
Stomach cancer	3
Esophageal cancer	2

Notes: Data are number of patients/lesions, with percentages in parentheses, except for age, which is years.

Diagnostic efficacy of MRI in finding the malignancy

MRI scans were accomplished in all the 116 VCFs, and the Gd-DTPA contrast-enhanced MRI was carried out in 83 VCFs, in which 35 of the 41 VCFs ultimately determined to be malignant and in 48 of the 75 VCFs ultimately determined to be benign. The three MRI features for malignant VCF were epidural mass formation, convex posterior cortex, and pedicle enhancement (Figure 1). Among the 41 malignant VCFs, epidural mass formation was observed in 34 cases (82.9%), convex posterior cortex was observed in 31 cases (75.6%), and pedicle enhancement was seen in 30 of the 35 cases (85.7%) in whom contrast-enhanced MRI was obtained. On the other hand, epidural mass formation was seen in 14 of the 75 (18.7%) benign VCFs, convex posterior cortex was seen in 17 (22.7%) cases, and pedicle enhancement was seen in 14 of the 48 (29.2%) cases in whom contrast-enhanced MRI

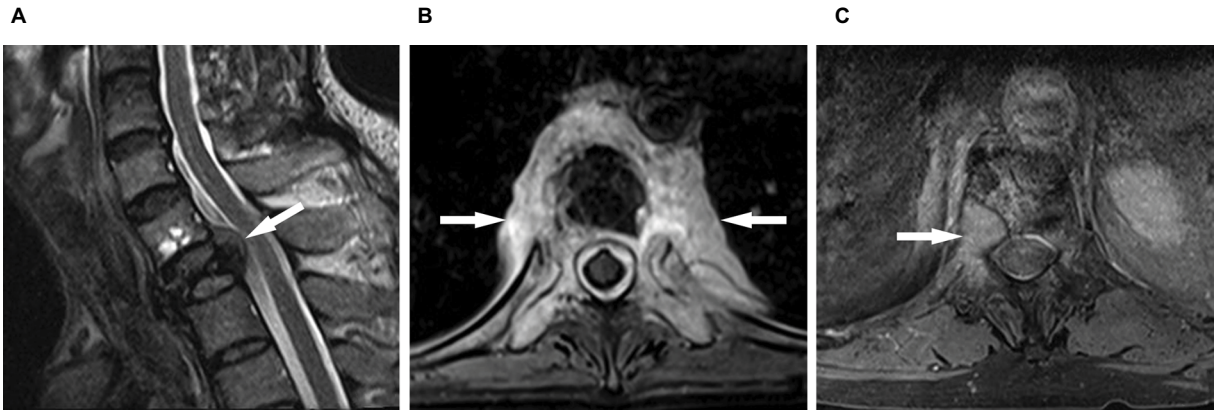

Figure 1 Three typical morphological features implying malignancy on MRI. (**A**) Convex posterior cortex (arrow indicated) on sagittal view; (**B**) epidural mass formation (arrow indicated) on axial view; and (**C**) pedicle enhancement (arrow indicated) on Gd-DTPA enhanced axial view.
Abbreviations: Gd-DTPA, a gadolinium-based MRI contrast agent; MRI, magnetic resonance imaging.

was obtained. Regarding the feature of epidural mass formation, the sensitivity, specificity, PPV, and NPV were 82.9%, 81.3%, 70.8%, and 89.7%, respectively. For the feature of convex posterior cortex, a sensitivity of 75.6%, specificity of 77.3%, PPV of 64.6%, and NPV of 85.3% were noted. For pedicle enhancement, the sensitivity, specificity, PPV, and NPV were 85.7%, 70.8%, 68.2%, and 87.2%, respectively. Of the three MRI features for malignancy, pedicle enhancement was the most sensitive diagnostic feature and epidural mass formation was the most specific feature. The simultaneous presence of all the three malignant findings were seen in 19 of the 35 malignant VCFs, and benign VCFs included all the three features that were observed only in 3 of the 48 patients, thereby the sensitivity and specificity for all the three features were 54.2% and 93.8%, respectively. The diagnostic efficacy of all the three malignant findings on MRI has been summarized in Figure 2 and in Table 2.

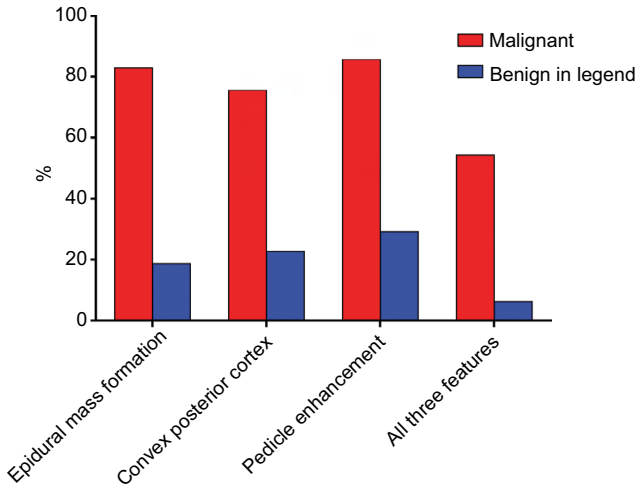

Figure 2 Column diagram shows the relative incidence of three MRI malignant findings in malignant and benign vertebral compression fractures.
Abbreviation: MRI, magnetic resonance imaging.

Diagnostic efficacy of ^{18}F-FDG PET/CT in finding the malignancy

^{18}F-FDG PET/CT scans were performed in 51 patients, in which 37 patients were with 41 malignant VCFs and 14 patients were with 18 benign VCFs. Increased ^{18}F-FDG uptake (lesion SUV_{max} is greater than that in the liver) was observed in all the 41 malignant VCFs (Figure 3) and in 11 of the benign VCFs (Figure 4). As such, the sensitivity and specificity of ^{18}F-FDG PET/CT for malignant VCFs were 100% and 38.9%, respectively (Table 2). In other words, the VCF lesion can be considered to be benign when only mild or no ^{18}F-FDG uptake is observed on the PET/CT image. Regarding the 41 malignant VCFs investigated, the SUV_{max} values were between 2.6 and 9.3, and the mean value was 5.0 ± 1.8. The SUV_{max} in the 18 benign VCFs ranged from 1.7 to 4.9, and the mean value was 2.9 ± 1.0. A significant difference regarding the mean SUV_{max} values was observed between the benign and malignant VCF lesions ($P < 0.001$) (Figure 5A). The most discriminative cutoff value of SUV_{max} was observed using ROC methodology which optimized the specificity and sensitivity to obtain the highest accuracy. The optimal cutoff value of SUV_{max} was 3.45 (the AUC value is 0.865; $P < 0.001$), which has a sensitivity of 82.9% and a specificity of 77.8% for determining the malignant VCFs (Figure 5B). Besides the value of SUV_{max}, the FDG uptake pattern within the VCFs differed in benign and malignant lesions. In the group of benign VCFs, the "striped" ^{18}F-FDG uptake was observed within the cortical bone or adjacent soft tissue around the fracture in 16 of the 18 cases (88.9%), and there was no uptake in the region of bone marrow. Conversely, in

Table 2 Diagnostic efficacy of MRI and ^{18}F-FDG PET/CT in finding the malignancy in all patients

Feature	Group		Sensitivity (%)	Specificity (%)	PPV	NPV
	Malignant fracture	Benign fracture				
Epidural mass formation	34/41	14/75	82.9	81.3	70.8	89.7
Convex posterior cortex	31/41	17/75	75.6	77.3	64.6	85.3
Pedicle enhancement	30/35	14/48	85.7	70.8	68.2	87.2
All three features	19/35	3/48	54.2	93.8	86.4	73.8
^{18}F-FDG PET/CT	41/41	11/18	100.0	38.9	90.1	100.0

Notes: Values represent number of lesions showing the specified feature/number of lesions evaluated. Group assignment was based on final diagnosis as determined by biopsy or clinical follow-up.

Abbreviations: PPV, positive predictive value; NPV, negative predictive value; ^{18}F-FDG, 2-[fluorine-18]-fluoro-2-deoxy-D-glucose; PET, positron emission tomography; CT, computed tomography.

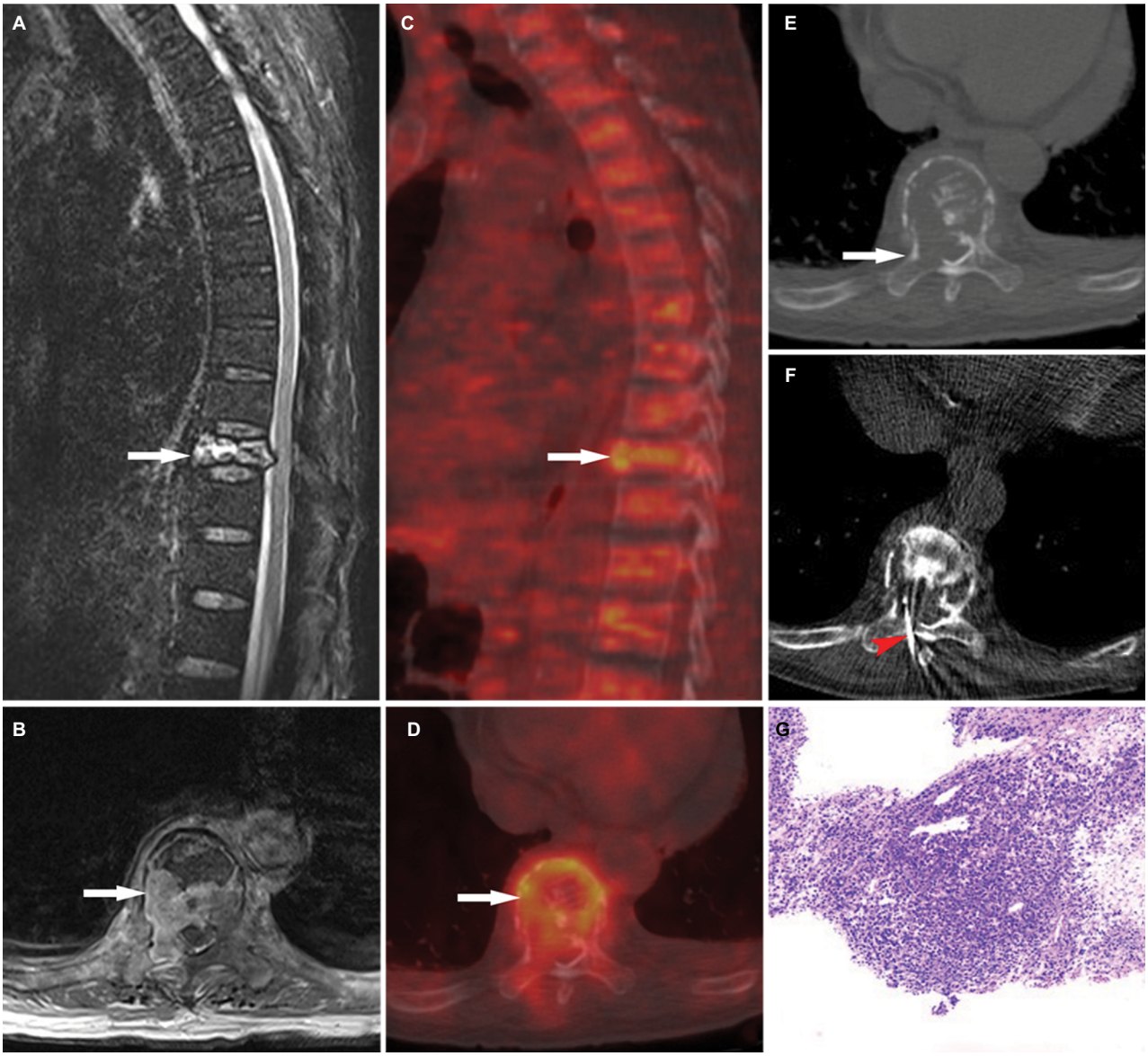

Figure 3 A 58-year-old man with compression fracture in the ninth thoracic vertebra (T9). (**A, B**) Magnetic resonance imaging shows the posterior cortical bulging on sagittal view (**A**, arrow indicated) and pedicle involvement on axial view (**B**, arrow indicated). (**C, D**) ^{18}F-FDG PET/CT imaging shows increased FDG uptake in the bone marrow (arrow indicated, SUV_{max} = 3.50). (**E, F**) CT-guided percutaneous biopsy is subsequently performed and the T9 lesion (arrow indicated) is chosen as the biopsy target (**E**). Axial noncontrast CT image shows the biopsy needle (red arrow indicated) positioned within the right side of the lesion (**F**). (**G**) Histological examination confirmed the bone lesion as the solitary plasma cell myeloma. Magnification ×100.

Abbreviations: ^{18}F-FDG, 2-[fluorine-18]-fluoro-2-deoxy-D-glucose; PET, positron emission tomography; CT, computed tomography; $SUV_{max,}$ maximum standardized uptake value.

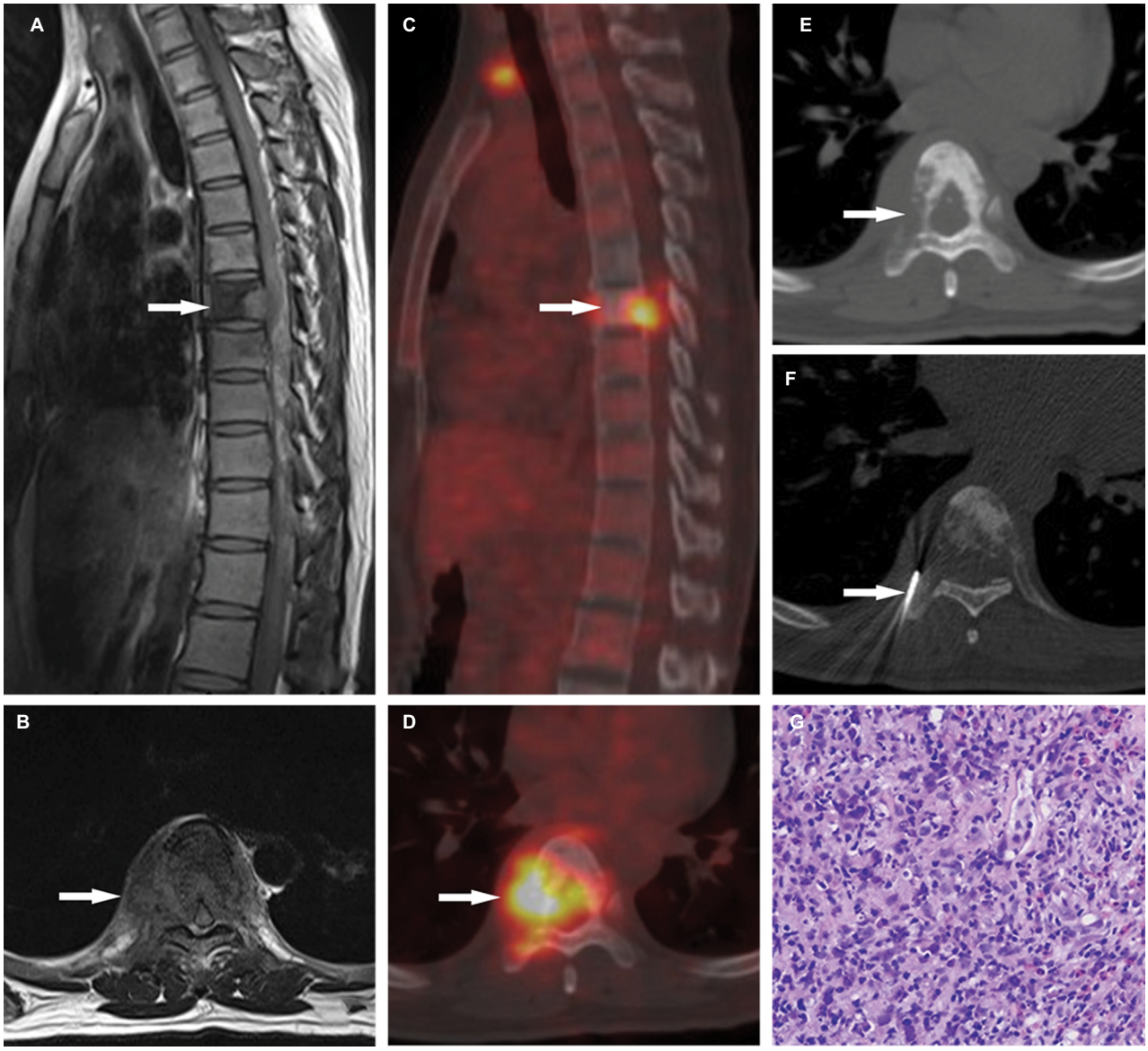

Figure 4 A 62-year-old woman with compression fracture in the sixth thoracic vertebra (T6). **(A, B)** Magnetic resonance imaging shows the posterior cortical bulging on sagittal view (**A**, arrow indicated) and paraspinal mass formation on axial view (**B**, arrow indicated). **(C, D)** ^{18}F-FDG PET/CT imaging shows increased FDG uptake in the soft tissue adjacent to T6 (arrow indicated, SUV_{max} = 4.90). **(E, F)** CT-guided percutaneous biopsy is subsequently performed and the T6 paraspinal mass (arrow indicated) is chosen as the biopsy target (**E**). Axial noncontrast CT image shows the biopsy needle (arrow indicated) positioned within the right side of the paraspinal mass (**F**). **(G)** Histological examination showed presence of inflammatory infiltrates and interstitial expansion with no evidence of malignancy.

Abbreviations: ^{18}F-FDG, 2-[fluorine-18]-fluoro-2-deoxy-D-glucose; PET, positron emission tomography; CT, computed tomography; $SUV_{max,}$ maximum standardized uptake value.

the group of malignant VCFs, ^{18}F-FDG uptake was observed in the bone marrow in 37 of the 41 cases (90.2%), and the activity accumulation pattern was nodular (6/41, 14.6%), cord-shaped (19/41, 46.3%), or irregular (16/41, 39.1%), and no "striped" uptake was observed.

Diagnostic efficacy of finding the malignancy in patients with solitary VCF

For clinicians, there would be problems in handling the patients with solitary VCF. Considering this, in this study, the diagnostic efficacy of MRI and PET/CT in patients with solitary VCF was evaluated. Among the 57 patients with solitary VCF, 24 of them were ultimately determined to be malignant, whereas the other 33 patients were determined to be benign. The diagnostic efficacy of MRI for patients with solitary VCF has been summarized in Table 3, and similar results could be observed in all the patients.^{18}F-FDG PET/CT scans were performed in 43 patients with solitary VCF, in which 33 patients were with malignant VCFs and the other 10 patients were with benign VCFs. The sensitivity

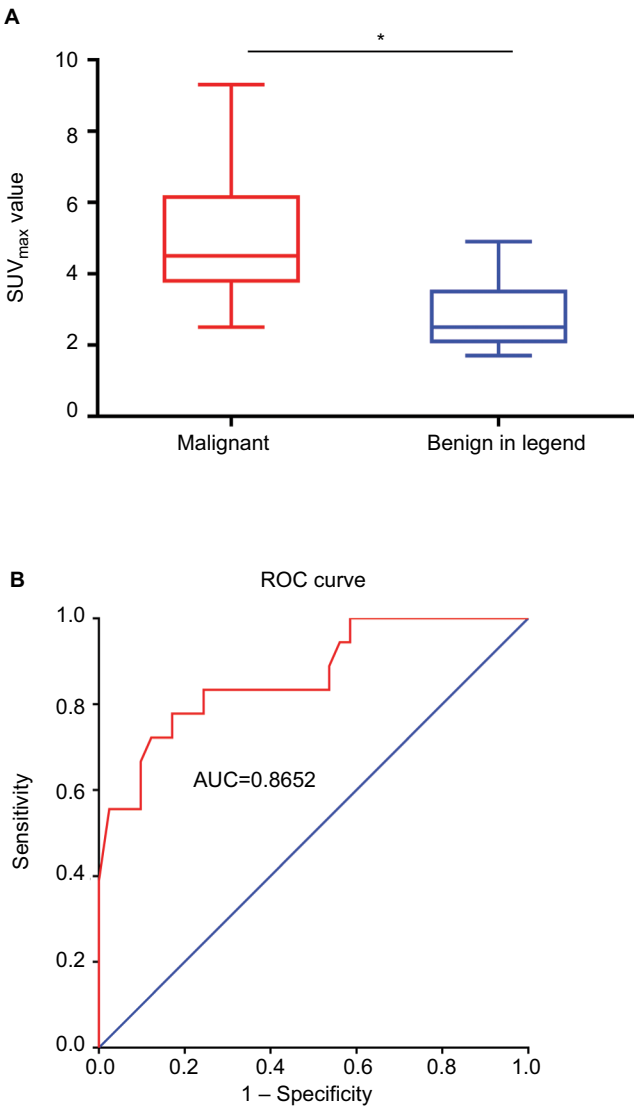

Figure 5 **(A)** Box plot of FDG SUV_{max} from malignant and benign vertebral compression fractures (VCFs). Bottom and top of each box are lower and upper quartiles. The band near middle of box is median. Extremes of lower and higher whiskers represent range of minimum and maximum values. *$P<0.05$, Wilcoxon signed-rank test. **(B)** Receiver operating characteristic (ROC) curve analysis was performed to calculate the optimal cutoff value of SUV_{max} for the differentiation between benignity and malignancy. Sensitivity and specificity changed with changes in the SUV_{max}. The SUV_{max} of the farthest point away from the chance line was 3.45.
Abbreviations: ^{18}F-FDG, 2-[fluorine-18]-fluoro-2-deoxy-D-glucose; SUV_{max}, maximum standardized uptake value; AUC, area under the curve.

and specificity of ^{18}F-FDG PET/CT for malignant VCFs were 100% and 40.0%, respectively (Table 3). Significant difference with respect to mean SUV_{max} values was observed between the benign and malignant VCF lesions (5.1 ± 1.8 vs 3.3 ± 1.1, $P < 0.001$). For patients with solitary benign VCFs, the "striped" ^{18}F-FDG uptake was observed within the cortical bone or adjacent soft tissue around the fracture in all the 10 cases (100.0%) and there was no uptake in the region of bone marrow. Conversely, for patients with solitary malignant VCFs, ^{18}F-FDG uptake was observed in the bone marrow in 32 of the 33 cases (97.0%).

Discussion

If a VCF occurs without any obvious symptoms, a further search on the reasons is crucial, in order to eliminate the possibility of malignant disease. VCFs may occur due to many reasons, such as metastasis, plasma cell myeloma, osteoporosis, or inflammatory disease. It has been reported that about 30% of VCFs occurring in patients with known malignant tumours are benign.[14] Thus, it is very important to differentiate the fractures of benign from malignant, particularly in osteoporotic patients with a history of neoplasms, in order to guide therapeutic strategies and for prognosis.

MRI has been widely regarded as the first-line imaging modality for the evaluation of VCFs. According to a series of MRI studies,[4,15,16] typical findings for malignancy include 1) convex posterior cortex, 2) epidural mass formation, and 3) high or inhomogeneous signal intensity within the vertebral body after Gd-DTPA injection. Cho and Chang analyzed 96 patients with 102 VCFs (35 malignant and 67 benign lesions), and concluded that the sensitivity and specificity for malignant compression fractures were 74.3% and 55.2% for convex posterior cortex, 77.1% and 74.6% for epidural mass formation, and 90.9% and 60.9% for pedicle enhancement.[17] Another study performed by Reinartz et al included 35 patients with pathological vertebral fractures and 23 patients with osteoporotic vertebral fractures.[18] In

Table 3 Diagnostic efficacy of MRI and ^{18}F-FDG PET/CT in finding the malignancy in patients with solitary VCF

Feature	Group		Specificity (%)	PPV	NPV
	Malignant fracture	Benign fracture			
Epidural mass formation	25/33	6/24	75.0	80.6	69.2
Convex posterior cortex	21/33	5/24	79.1	80.7	61.2
Pedicle enhancement	23/27	6/20	70.0	79.3	77.8
All three features	14/27	2/20	90.0	87.5	58.0
^{18}F-FDG PET/CT	33/33	6/10	40.0	84.7	100.0

Notes: Values represent number of lesions showing the specified feature/number of lesions evaluated. Group assignment was based on final diagnosis as determined by biopsy or clinical follow-up.
Abbreviations: VCF, vertebral compressed fracture; PPV, positive predictive value; NPV, negative predictive value; ^{18}F-FDG, 2-[fluorine-18]-fluoro-2-deoxy-D-glucose; PET, positron emission tomography; CT, computed tomography.

this study, they suggested that the pedicle involvement was the most significant finding for identifying the malignancy (sensitivity of 91.4% and a specificity of 82.6%) among the three malignant findings using MRI. A combination of two or more MRI findings provided higher specificity and PPV. In our study, the sensitivity and specificity for identifying the malignant VCFs were 75.6% and 77.3% for convex posterior cortex, 82.9% and 81.3% for epidural mass formation, and 85.7% and 70.8% for pedicle enhancement (Figure 2 and Table 2). Based on our results, the pedicle enhancement is determined to be suggestive of, but not specific, in evaluating the malignant VCFs. The outcome of such a finding in benign VCFs may be explained by the minimal bleeding or the formation of soft tissue edema around the osteoporotic vertebral fractures. It is also worth noting that the simultaneous occurrence of three malignant findings demonstrated a specificity of 93.8%, which was higher than the sensitivity from any single MRI finding. However, the occurrence of three features resulted in low sensitivity (54.2%). Therefore, the differentiation between benign and malignant fractures cannot always be possible by MR images. Additional MR sequences such as fat-suppressed T2-weighted imaging, DWI, or Dixon MRI sequence may be helpful for clear delineation.[8,19]

^{18}F-FDG PET has been widely used for detecting the spinal metastases in cancer patients.[20] Based on Fogelman's investigation,[21] ^{18}F-FDG PET and bone scintigraphy showed a similar sensitivity for the detection of spinal metastases (77%), but ^{18}F-FDG PET was more specific (97% vs 81%). This is because the osteoblastic response caused by osteoporosis or chronic trauma may be less likely to be detected by ^{18}F-FDG PET. Recently, few studies indicated that FDG PET/CT seemed to be able to differentiate the pathological fractures from benign fractures based on the SUV_{max} from vertebral bodies, and the SUV_{max} value along with CT characteristics of the lesions (such as mass formation in the paravertebral soft tissue and spinal accessory involvement) should further enhance the diagnostic accuracy of ^{18}F-FDG PET/CT.[22,23] Bredella et al have reported the sensitivity, specificity, PPV, NPV, and accuracy of ^{18}F-FDG PET/CT in the differentiation between benign and malignant VCFs were 86%, 83%, 84%, 71%, and 92%, respectively. The SUV_{max} values from malignant fractures (mean SUV_{max}: 3.9 ± 1.52) were significantly higher than those from benign fractures (mean SUV_{max}: 1.9 ± 0.97) ($P < 0.01$), but there was no statistical difference with respect to SUV_{max} between acute and chronic benign fractures.[24] A study reported by Kato et al indicated that FDG-PET could be a useful method for early differentiation between acute benign and metastatic fractures, where acute benign fractures did not show any significant FDG uptake (SUV_{max} ranged between 0.2 and 1.1).[25] Zhuang et al reported that a traumatic fracture or orthopedic intervention may show an acutely increased FDG accumulation, with SUV_{max} ranging from 1.1 to 2.4 (mean value = 1.7). However, this finding was not likely to remain for longer than 3 months under normal circumstances.[26]

In this study, ^{18}F-FDG PET/CT demonstrated a higher sensitivity but lower specificity as compared to MRI with respect to the differentiation between benign and malignant VCFs (Table 2). It is also observed that ^{18}F-FDG PET/CT demonstrated no uptake or only slightly increased uptake in the osteoporotic fractures (SUV_{max}: 1.7–4.9; mean value: 2.9 ± 1.0), while a higher FDG uptake often reflected malignant processes (SUV_{max}: 2.6–9.3; mean value: 5.0 ± 1.8). Besides the value of SUV_{max}, it was noticed that the ^{18}F-FDG uptake pattern was very different between malignant and benign compressed fractures. In malignant fractures, ^{18}F-FDG uptake was mostly observed in the region of bone marrow with a relatively high SUV_{max} (Figure 3), and the accumulation pattern was nodular, cord-shaped, or irregular. Regarding the benign fractures, "striped" FDG uptake was mostly observed in the region of cortical bone or adjacent soft tissue around the fracture, but rarely found out in the marrow (Figure 4). Such a finding may be explained by the different fracture formation modes and pathological processes between benign and malignant fractures. Benign fracture is caused by an exogenous process and thus the accumulation pattern reflects the inflammatory reaction along the fracture line. Whereas, the malignant fracture is mainly due to cancer metastasis which caused the destruction of bone, and the accumulation pattern of FDG reflects the characteristics of bone metastases. Therefore, regarding the delineation of malignant VCFs from ^{18}F-FDG PET/CT, the FDG uptake pattern should also be considered in addition to the value of SUV_{max}. Moreover, our study suggested an optimal cutoff value of SUV_{max} for differentiating the lesions of malignant from benign to be 3.45, which has the sensitivity of 82.9% and specificity of 77.8% for identifying malignancy (Figure 5). As compared with the simultaneous occurrence of three malignant findings on MRI, SUV_{max} showed a much higher sensitivity (82.9% vs 54.2%), but a slightly lower specificity (77.8% vs 93.8%). Regarding the purpose of screening for metastases, the sensitivity is more important as compared to specificity as the false-negative results may lead to severe consequences for the patients.

For clinicians, there would be problems in handling the patients with solitary VCF. Considering this, in this study, the diagnostic efficacy of MRI and PET/CT in patients with solitary VCF was evaluated. The diagnostic efficacy of MRI for patients with solitary VCF was similar to the results as observed in all the patients (Table 3). Regarding the diagnostic efficacy of PET/CT, a significant difference could also be observed for the SUV_{max} values between the benign and malignant groups (5.1 ± 1.8 vs 3.3 ± 1.1, $P < 0.001$). However, it is interesting to find that the difference in the uptake pattern of FDG was even more significant. For patients with solitary benign VCFs, the "striped" ^{18}F-FDG uptake was found to be observed within the cortical bone or adjacent soft tissue around the fracture in all the cases (100.0%). For patients with solitary malignant VCFs, ^{18}F-FDG uptake was observed to be in the bone marrow in most of the cases (32/33, 97.0%). Therefore, for patients with solitary VCF, ^{18}F-FDG uptake pattern may be especially important as it provides key information for differentiating the fractures of benign from malignancy.

Based on the results obtained from our investigation, a diagnostic algorithm has been proposed for patients with VCFs. MRI is still the first-line diagnostic imaging modality and should be initially performed. It is not recommended to use ^{18}F-FDG PET/CT for the screening, but rather as a complementary imaging modality only in problematic cases. In a situation where all the three malignant features are observed on MRI, such VCFs are highly suspicious of malignancy and biopsy should be subsequently performed. In a situation where one or two malignant features are observed on MRI, ^{18}F-FDG PET/CT is recommended for further diagnosis. If the VCF lesion showed no or mild FDG uptake and/or FDG uptake was observed in the region of cortical bone or in the adjacent soft tissue around the fracture, this is suggestive of a benign lesion and a further observation or follow-up imaging could be considered. If the VCF lesion showed a positive PET result and FDG uptake was observed in the region of bone marrow, a high probability for malignant VCF should be considered and biopsy should be subsequently performed. In cases where no malignant features are observed on MRI, the VCF lesion could be considered to be benign.

Finally, there are some limitations which should be noted in this study. Firstly, the optimal cutoff value of SUV_{max} as suggested is generated from a single-center retrospective study. Such a SUV_{max} value cannot be used as a general threshold for differentiating the lesions of malignant from benign. The recommended SUV_{max} threshold for practice required multicenter study with a large population. Additionally, in this study, the MR imaging protocol primarily used T1 and T2 sequences for the evaluation of VCFs, and additional sequences (such as DWI) were not routinely performed in spine MRI. Our MR imaging protocol may not represent the standard MR imaging protocol in other hospitals and this may call into concern the accuracy of the outcomes for the MRI evaluation group.

Conclusion

Significant findings from MRI which include convex posterior cortex, epidural mass formation, and pedicle enhancement are highly suggestive of malignancy. ^{18}F-FDG PET/CT reliably differentiated the fractures of malignant from benign based on both SUV_{max} and ^{18}F-FDG uptake pattern. Compared with MRI, ^{18}F-FDG PET/CT demonstrated a higher sensitivity but a lower specificity with respect to the differentiation between benign and malignant VCFs. Therefore, in a situation where MRI findings are not diagnostic, ^{18}F-FDG PET/CT could provide additional information as it has high sensitivity and is semiquantitative.

Acknowledgment

This study was supported by the Natural Science Foundation of China (81701736), the Natural Science Foundation of Fujian Province of China (No 2015J01543; 2016J01642) and Fujian Middle-aged Backbone Talents Program (2017-ZQN-82).

Author contributions

XH and LZ contributed to the conception and design of the study. XG, LZ, JW, and JH provided patient data and clinical support. XH, XG, and CX drafted the manuscript. LS and HC carried out guidance and supervision for the work and modified the paper. All authors contributed toward data analysis, drafting and critically revising the paper and agree to be accountable for all aspects of the work. All authors read and approved the final manuscript.

Disclosure

The authors report no conflicts of interest in this work.

References

1. Alexandru D, So W. Evaluation and management of vertebral compression fractures. *Perm J*. 2012;16(4):46–51.
2. Shah LM, Salzman KL. Imaging of spinal metastatic disease. *Int J Surg Oncol*. 2011;2011:769753.
3. Even-Sapir E. Imaging of malignant bone involvement by morphologic, scintigraphic, and hybrid modalities. *J Nucl Med*. 2005;46(8):1356–1367.
4. Cicala D, Briganti F, Casale L, et al. Atraumatic vertebral compression fractures: differential diagnosis between benign osteoporotic and malignant fractures by MRI. *Musculoskelet Surg*. 2013;97(Suppl 2):S169–S179.

5. Lipton A, Uzzo R, Amato RJ, et al. The science and practice of bone health in oncology: managing bone loss and metastasis in patients with solid tumors. *J Natl Compr Canc Netw*. 2009;7(Suppl 7):S1–29; quiz S30.
6. Yuh WT, Zachar CK, Barloon TJ, Sato Y, Sickels WJ, Hawes DR. Vertebral compression fractures: distinction between benign and malignant causes with MR imaging. *Radiology*. 1989;172(1):215–218.
7. Wood KB, Li W, Lebl DR, Ploumis A. Management of thoracolumbar spine fractures. *Spine J*. 2014;14(1):145–164.
8. Park HJ, Lee SY, Rho MH, et al. Single-shot echo-planar diffusion-weighted MR imaging at 3T and 1.5T for differentiation of benign vertebral fracture edema and tumor infiltration. *Korean J Radiol*. 2016;17(5):590–597.
9. Castillo M. Diffusion-weighted imaging of the spine: is it reliable? *AJNR Am J Neuroradiol*. 2003;24(6):1251–1253.
10. Geith T, Schmidt G, Biffar A, et al. Comparison of qualitative and quantitative evaluation of diffusion-weighted MRI and chemical-shift imaging in the differentiation of benign and malignant vertebral body fractures. *AJR Am J Roentgenol*. 2012;199(5):1083–1092.
11. Freebody J, Wegner EA, Rossleigh MA. 2-deoxy-2-((18)F)fluoro-D-glucose positron emission tomography/computed tomography imaging in paediatric oncology. *World J Radiol*. 2014;6(10):741–755.
12. Abo-Sheisha DM, Badawy ME. The diagnostic value of PET/CT in recurrence and distant metastasis in breast cancer patients and impact on disease free survival. *Egypt J Radiol Nuclear Med*. 2014;45(4):1317–1324.
13. Chen H, Niu G, Wu H, Chen X. Clinical application of radiolabeled RGD peptides for PET imaging of integrin alphavbeta3. *Theranostics*. 2016;6(1):78–92.
14. Hamimi A, Kassab F, Kazkaz G. Osteoporotic or malignant vertebral fracture? This is the question. What can we do about it? *Egypt J Radiol Nuclear Med*. 2015;46(1):97–103.
15. Sung JK, Jee WH, Jung JY, et al. Differentiation of acute osteoporotic and malignant compression fractures of the spine: use of additive qualitative and quantitative axial diffusion-weighted MR imaging to conventional MR imaging at 3.0 T. *Radiology*. 2014;271(2):488–498.
16. Thawait SK, Marcus MA, Morrison WB, Klufas RA, Eng J, Carrino JA. Research synthesis: what is the diagnostic performance of magnetic resonance imaging to discriminate benign from malignant vertebral compression fractures? Systematic review and meta-analysis. *Spine (Phila Pa 1976)*. 2012;37(12):E736–E744.
17. Cho WI, Chang UK. Comparison of MR imaging and FDG-PET/CT in the differential diagnosis of benign and malignant vertebral compression fractures. *J Neurosurg Spine*. 2011;14(2):177–183.
18. Reinartz P, Schaffeldt J, Sabri O, et al. Benign versus malignant osseous lesions in the lumbar vertebrae: differentiation by means of bone SPET. *Eur J Nucl Med*. 2000;27(6):721–726.
19. Kim DH, Yoo HJ, Hong SH, Choi JY, Chae HD, Chung BM. Differentiation of acute osteoporotic and malignant vertebral fractures by quantification of fat fraction with a Dixon MRI sequence. *AJR Am J Roentgenol*. 2017;209(6):1331–1339.
20. Metser U, Lerman H, Blank A, Lievshitz G, Bokstein F, Even-Sapir E. Malignant involvement of the spine: assessment by 18F-FDG PET/CT. *J Nucl Med*. 2004;45(2):279–284.
21. Fogelman I, Cook G, Israel O, Van der Wall H. Positron emission tomography and bone metastases. *Semin Nucl Med*. 2005;35(2):135–142.
22. Shin DS, Shon OJ, Byun SJ, Choi JH, Chun KA, Cho IH. Differentiation between malignant and benign pathologic fractures with F-18-fluoro-2-deoxy-D-glucose positron emission tomography/computed tomography. *Skeletal Radiol*. 2008;37(5):415–421.
23. Hamaoka T, Madewell JE, Podoloff DA, Hortobagyi GN, Ueno NT. Bone imaging in metastatic breast cancer. *J Clin Oncol*. 2004;22(14):2942–2953.
24. Bredella MA, Essary B, Torriani M, Ouellette HA, Palmer WE. Use of FDG-PET in differentiating benign from malignant compression fractures. *Skeletal Radiol*. 2008;37(5):405–413.
25. Kato K, Aoki J, Endo K. Utility of FDG-PET in differential diagnosis of benign and malignant fractures in acute to subacute phase. *Ann Nucl Med*. 2003;17(1):41–46.
26. Zhuang H, Sam JW, Chacko TK, et al. Rapid normalization of osseous FDG uptake following traumatic or surgical fractures. *Eur J Nucl Med Mol Imaging*. 2003;30(8):1096–1103.